

1 **Interpreting UniFrac with Absolute Abundance: A Conceptual and Practical Guide**

2 Augustus Pendleton^{1*} & Marian L. Schmidt^{1*}

3 ¹Department of Microbiology, Cornell University, 123 Wing Dr, Ithaca, NY 14850, USA

4 **Corresponding Authors:** Augustus Pendleton: arp277@cornell.edu; Marian L. Schmidt:
5 marschmi@cornell.edu

6 **Author Contribution Statement:** Both authors contributed equally to the manuscript.

7 **Preprint servers:** This article was submitted to *bioRxiv* (doi: 10.1101/2025.07.18.665540) under
8 a CC-BY-NC-ND 4.0 International license.

9 **Keywords:** Microbial Ecology - Beta Diversity - Absolute Abundance - Bioinformatics -
10 UniFrac

11 **Data Availability:** All data and code used to produce the manuscript are available at
12 https://github.com/MarschmiLab/Pendleton_2025_Absolute_Unifrac_Paper, in addition to a
13 reproducible renv environment. All packages used for analysis are listed in Table S1.

14

Formatted: Font: Bold

Formatted: Line spacing: single

15 **Abstract**

16 β -diversity is central to microbial ecology, yet commonly used metrics overlook changes in
17 microbial load, limiting their ability to detect ecologically meaningful shifts. Popular for
18 incorporating phylogenetic relationships, UniFrac distances currently default to relative
19 abundance and therefore omit important variation in microbial abundances. As quantifying
20 absolute abundance becomes more accessible, integrating this information into β -diversity
21 analyses is essential. Here, we introduce *Absolute UniFrac* (GU^A), a variant of Weighted UniFrac
22 that incorporates absolute abundances. Using simulations and a reanalysis of four 16S rRNA
23 metabarcoding datasets (from a nuclear reactor cooling tank, the mouse gut, a freshwater lake,
24 and the peanut rhizosphere), we demonstrate that *Absolute UniFrac* captures microbial load,
25 composition, and phylogenetic relationships. While this can improve statistical power to detect
26 ecological shifts, we also find *Absolute UniFrac* can be strongly correlated to differences in cell
27 abundances alone. To balance these effects, we also incorporate absolute abundance into the
28 generalized extension (GU^A) that has a tunable α parameter to adjust the influence of abundance
29 and composition. Finally, we benchmark GU^A and show that although computationally slower
30 than conventional alternatives, GU^A is comparably insensitive to realistic noise in load estimates
31 compared to conventional alternatives like Bray-Curtis dissimilarities, particularly at lower α . By
32 coupling phylogeny, composition, and microbial load, *Absolute UniFrac* integrates three
33 dimensions of ecological change, better equipping microbial ecologists to quantitatively compare
34 microbial communities.

Deleted: Microbial ecologists routinely use
Deleted: metrics to compare communities, yet these metrics vary in the ecological dimensions they capture.
Deleted: , omitting
Deleted: load
Deleted: methods for
Deleted: estimating
Deleted: gain traction, incorporating
Deleted: becomes
Deleted: present
Deleted: uses
Deleted: Through
Deleted: freshwater case study.
Deleted: show that
Deleted: captures both
Deleted: s
Deleted: ,
Deleted: ing
Deleted: .
Deleted: However, it is also sensitive to variation in microbial load, especially when abundance changes occur along long branches, potentially amplifying differences. We therefore recommend a...
Deleted: form
Deleted: with
Deleted: balance sensitivity and interpretability
Deleted: .
Deleted: ¶

63 **Main Text**

64 Microbial ecologists routinely compare communities using β -diversity metrics derived
 65 from relative abundances. Yet this approach overlooks a critical ecological dimension: microbial
 66 load. High-throughput sequencing produces compositional data, in which each taxon's
 67 abundance is constrained by all others [1]. However, quantitative profiling studies show that cell
 68 abundance, not only composition, can drive major community differences [2]. In low-biomass
 69 samples, relying on relative abundance can allow contaminants to appear biologically
 70 meaningful despite absolute counts too low for concern [3].

Deleted:

71 Sequencing-based microbiome studies therefore rely on relative abundance even when
 72 the hypotheses of interest implicitly concern absolute changes in biomass. This creates a
 73 mismatch between ecological framing (growth, bloom magnitude, pathogen proliferation,
 74 disturbance recovery, or colonization pressure) and the information the β -diversity metric
 75 encodes [4]. As a result, β -diversity is often treated as if it includes biomass, even when absolute
 76 abundance is either not measured at all or is measured but excluded from the calculation (as in
 77 conventional UniFrac). Many studies therefore test biomass-linked hypotheses using a metric
 78 that normalizes biomass away [4]. A conceptual correction is needed in which β -diversity is
 79 understood as variation along three axes: composition, phylogeny and absolute abundance.

Deleted: {Citation}

80 Absolute microbial load measurements are now increasingly obtainable through flow
 81 cytometry, qPCR, and genomic spike-ins, allowing biomass to be quantified alongside taxonomic
 82 composition [4, 5]. These approaches improve detection of functionally relevant taxa and
 83 mitigate the compositional constraints imposed by sequencing [1, 2]. Most studies that
 84 incorporate absolute abundance counts currently rely on Bray-Curtis dissimilarity, which can
 85 capture load but does not consider phylogenetic similarity [5–7]. UniFrac distances provide the
 86 opposite strength, incorporating phylogeny but discarding absolute abundance, as they are
 87 restricted to relative abundance data by construction [8]. This leaves no phylogenetically
 88 informed β -diversity metric that operates on absolute counts, despite the fact that biomass is
 89 central to many ecological hypotheses.

Deleted: 1

To overcome compositional constraints, researchers increasingly use

Deleted: to quantify microbial load**Deleted:** tools**Deleted:** using**Deleted:** dat**Deleted:** a have used**Deleted:** does not necessarily expect normalization to proportions**Formatted:** Font: Italic

Deleted: But in the field of microbial ecology, UniFrac distances remain popular when working with relative abundance data. Here, we present *Absolute UniFrac*, a direct extension of Weighted UniFrac that incorporates total abundance, and evaluate its impact across simulated and real-world datasets.

90 To evaluate the implications of incorporating absolute abundance into phylogenetic β -
 91 diversity, we use both simulations and reanalysis of four 16S rRNA amplicon datasets. The
 92 simulations use a simple four-taxon community with controlled abundance shifts to directly
 93 compare both Bray-Curtis and UniFrac in their relative and absolute forms, illustrating how each
 94 metric responds when abundance, composition, or evolutionary relatedness differ. We then
 95 reanalyze four real-world datasets spanning nuclear reactor cooling water [5], the mouse gut [3],
 96 a freshwater lake [9], and rhizosphere soil [10]. These differ widely in richness, biomass range,
 97 and ecological context, allowing us to test when absolute abundance changes align with or
 98 diverge from phylogenetic turnover. Together, these simulations and reanalyses provide the
 99 empirical foundation for interpreting *Absolute UniFrac* relative to existing β -diversity measures
 100 across the three axes of ecological difference: abundance, composition, and phylogeny.

Formatted: Indent: First line: 0.5", Line spacing: single

101 We also extend *Absolute UniFrac* as was proposed by [11] to Generalized *Absolute*
 102 *UniFrac* that incorporates a tunable ecological dimension, α , and evaluate its impact across
 103 simulated and real-world datasets. As α increases, β -diversity is increasingly correlated with
 104 differences in absolute abundance, allowing researchers to fine tune the relative weight their
 105 analyses place on microbial load versus composition.

124 **Defining Absolute UniFrac**

125 The UniFrac distance was first introduced by Lozupone & Knight (2005) and has since
 126 become enormously popular as a measure of β -diversity within the field of microbial ecology
 127 [12]. A benefit of the UniFrac distance is that it considers phylogenetic information when
 128 estimating the distance between two communities. After first generating a phylogenetic tree
 129 representing species (or amplicon sequence variants, “ASVs”) from all samples, the UniFrac
 130 distance computes the fraction of branch-lengths which is *shared* between communities, relative
 131 to the total branch length represented in the tree. UniFrac can be both unweighted, in which only
 132 the incidence of species is considered, or weighted, wherein a branch’s contribution is weighted
 133 by the proportional abundance of taxa on that branch [8]. The Weighted UniFrac is derived:

$$U^R = \frac{\sum_{i=1}^n b_i |p_i^a - p_i^b|}{\sum_{i=1}^n b_i (p_i^a + p_i^b)}$$

134 where the contribution of each branch length, b_i , is weighted by the difference in the relative
 135 abundance of all species (p_i) descended from that branch in sample a or sample b . Here, we
 136 denote this distance as U^R , for “Relative UniFrac”. Popular packages which calculate weighted
 137 UniFrac—including the diversity-lib QIIME plug-in and the R packages phyloseq and
 138 GUniFrac—run this normalization by default [11, 13, 14].

139
 140 Importantly, U^R is most sensitive to changes in abundant lineages, which can sometimes
 141 obscure compositional differences driven by rare to moderately-abundant taxa [11]. To address
 142 this weakness, Chen et al. (2012) introduced the generalized UniFrac distance (GU^R), in which
 143 the impact of abundant lineages can be mitigated by decreasing the parameter α :

$$GU^R = \frac{\sum_{i=1}^n b_i (p_i^a + p_i^b)^\alpha |p_i^a - p_i^b|}{\sum_{i=1}^n b_i (p_i^a + p_i^b)^\alpha}$$

144 where α ranges from 0 (close to Unweighted UniFrac) up to 1 (identical to U^R , above). However,
 145 if one wishes to use absolute abundances, both U^R and GU^R can be derived without normalizing
 146 to proportions:

$$U^A = \frac{\sum_{i=1}^n b_i |c_i^a - c_i^b|}{\sum_{i=1}^n b_i (c_i^a + c_i^b)} \quad GU^A = \frac{\sum_{i=1}^n b_i (c_i^a + c_i^b)^\alpha |c_i^a - c_i^b|}{\sum_{i=1}^n b_i (c_i^a + c_i^b)^\alpha}$$

147 Where c_i^a and c_i^b denote for the absolute counts of species descending from branch b_i in
 148 communities a and b , respectively. We refer to these distances as *Absolute UniFrac* (U^A) and
 149 *Generalized Absolute UniFrac* (GU^A). Although substituting absolute for relative abundances is
 150 mathematically straightforward, we found no prior work that examines UniFrac in the context of
 151 absolute abundance, either conceptually or in application. Incorporating absolute abundances
 152 introduces a third axis of ecological variation: beyond differences in composition and
 153 phylogenetic similarity, U^A also captures divergence in microbial load. This makes interpretation
 154 of U^A nontrivial, particularly in complex microbiomes.

155 **Demonstrating β -diversity metrics’ behavior with a simple simulation**

156 Formatted: No underline
 Formatted: Line spacing: single

Deleted:

Formatted: Indent: First line: 0.5", Line spacing: single
 Deleted: s

Deleted: we weight the length

Deleted: f

Deleted: Because

Deleted: it

Formatted: Indent: First line: 0.5", Line spacing: single

Formatted: Line spacing: single

Deleted: stands

Deleted: ed

Deleted: y

Deleted: f

Deleted:

Deleted: U^A and

Formatted: No underline

Formatted: Font: Bold

170 To clarify how U^A behaves relative to existing β -diversity metrics, we first constructed a
171 simple four-taxon simulated community arranged in a small phylogeny (Fig. 1A). By varying the
172 absolute abundance of each ASV (1, 10, or 100), we generated 81 samples and 3,240 pairwise
173 comparisons. For each pair, we computed four dissimilarity metrics: Bray-Curtis with relative
174 abundance (BC^R), Bray-Curtis with absolute abundance (BC^A), Weighted UniFrac with relative
175 abundance (U^R), and Weighted UniFrac with absolute abundance (U^A). These comparisons help
176 to illustrate how each axis of ecological difference—abundance, composition, and phylogeny—is
177 expressed by the different metrics.

178 U^A does not consistently yield higher or lower distances compared to other metrics, but
179 instead varies depending on how abundance and phylogeny intersect (Fig. 1B). In the improbable
180 scenario that all branch lengths are equal, U^A is always less than or equal to BC^A (Fig. S1).
181 These comparisons emphasize that once branch lengths differ, incorporating phylogeny and
182 absolute abundance alters the structure of the distance space. The direction and magnitude of that
183 change depend on which branches carry the abundance shifts. U^A is also usually smaller than
184 BC^A and is more strongly correlated with BC^A (Pearson's $r = 0.82$, $p < 0.0001$) than with BC^R (r
185 = 0.41) and U^R ($r = 0.55$).

186 To better understand how these metrics diverge, we examined individual sample pairs
187 (Fig. 1C). Scenario 1 (gold star) illustrates the classic advantage of UniFrac: ASV_1 and ASV_2
188 are phylogenetically close, so U^R and U^A discern greater similarity between samples than BC^R
189 and BC^A , which ignore phylogenetic structure. Scenario 2 (red star) highlights a limitation of
190 relative metrics: two samples with identical relative composition but a 100-fold difference in
191 biomass appear identical to BC^R and U^R , but not to their absolute counterparts. In Scenario 3
192 (green star), incorporating absolute abundance decreases dissimilarity. BC^A and U^A are lower
193 than their relative counterparts because half the community is identical in absolute abundance,
194 even though their proportions differ. In contrast, Scenario 4 (blue star) shows that U^A can exceed
195 BC^A when abundance differences occur on long branches, amplifying phylogenetic dissimilarity.

196 These scenarios demonstrate that U^A integrates variation along three ecologically
197 relevant axes: composition, phylogenetic similarity, and microbial load, rather than isolating any
198 single dimension. Because a given U^A value can reflect multiple drivers of community change,
199 interpreting it requires downstream analyses to disentangle the relative contributions of these
200 three axes. To evaluate how this plays out in real systems we next reanalyzed four previously
201 published datasets spanning diverse microbial environments.

Formatted: Indent: First line: 0.5", Line spacing: single

Deleted: To illustrate how U^A behaves, we constructed a simulated community of four ASVs arranged in a simple phylogeny (Fig. 1A).

Deleted:

Deleted: reshapes distance estimates in nontrivial ways.

Deleted:

Deleted: terms, despite proportional differences

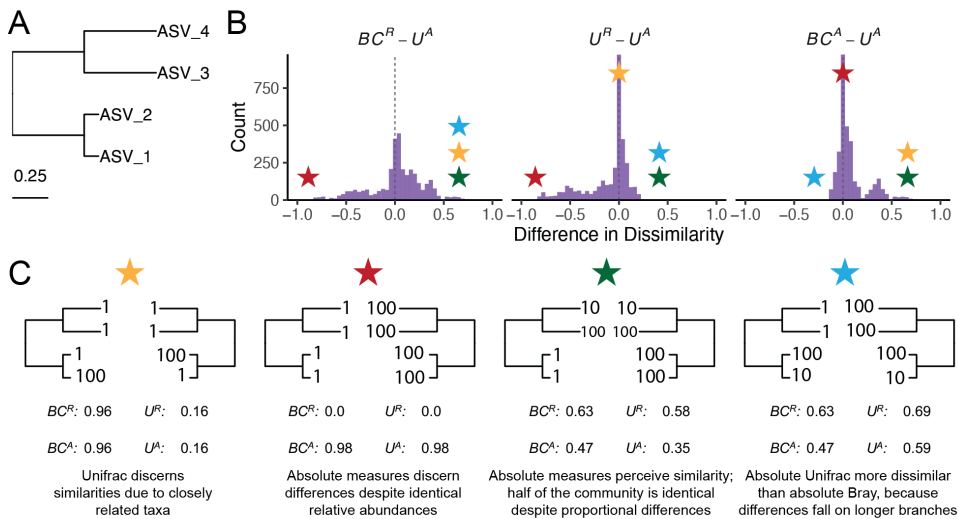
Deleted: increase dissimilarity relative to

Deleted: ¶

Formatted: Indent: First line: 0"

Formatted: Indent: First line: 0.5", Line spacing: single

Deleted: ¶



215 *Figure 1. Simulated communities reveal how absolute abundance affects phylogenetic and non-phylogenetic β -*
216 *diversity measures.* (A) We constructed a simple four-ASV community with a known phylogeny and generated all
217 permutations of each ASV having an absolute abundance of 1, 10, or 100, resulting in 81 unique communities and
218 3,240 pairwise comparisons. (B) Distributions of pairwise differences between weighted UniFrac using absolute
219 abundance (U^A) and three other metrics: Bray-Curtis using relative abundance (BC^R), weighted UniFrac using
220 relative abundance (U^R), and Bray-Curtis using absolute abundance (BC^A). (C) Illustrative sample pairs demonstrate
221 how absolute abundances and phylogenetic structure interact to increase or decrease dissimilarity across metrics.
222 Stars indicate where each scenario falls within the distributions shown in panel B. Actual values for each metric are
223 displayed beneath each scenario.

224 Application of Absolute UniFrac to Four Real-World Microbiome Datasets

225 To illustrate the sensitivity of U^A to both variation in composition and absolute
226 abundance, we re-analyzed four previously published datasets from diverse microbial systems.
227 These datasets included: (i) nuclear reactor cooling water sampled across three reactor cycle
228 phases [5]; (ii) the mouse gut sampled across multiple regions and between two diets [3]; (iii)
229 depth-stratified freshwater communities sampled across two months [9]; and (iv) peanut
230 rhizospheres under two crop rotation schemes (conventional rotation (CR) vs. sod-based rotation
231 (SBR)), plant maturities, and irrigation treatments [10]. Absolute abundance was quantified by
232 flow cytometry for the cooling water and freshwater datasets, droplet digital PCR for the mouse
233 gut, and by qPCR for the rhizosphere dataset. Together these span a wide range of richness—from
234 215 ASVs in the cooling water to 24,000 ASVs in the soil—and microbial load—from as low as
235 4×10^5 cells/ml (cooling water) up to 2×10^{12} 16S rRNA copies/gram (mouse gut). Additional

Formatted: Line spacing: single

Deleted: Example comparisons i

Deleted: ng specific scenarios where U^A yields greater or smaller dissimilarity than other metrics.

Deleted: Colored s

Deleted: Across all 3,240 pairwise comparisons, U^A is usually smaller than and strongly correlated with BC^A (Pearson's $r = 0.82$, $p < 0.0001$) than with BC^R ($r = 0.41$) and U^R ($r = 0.55$), reflecting the effect illustrated in Scenario 1. However, exceptions like Scenario 4 show that U^A can also yield larger distances than BC^A when abundance differences occur on long branches. These scenarios demonstrate that U^A

Formatted: Font: Bold

Formatted: Indent: First line: 0", Line spacing: single

248
249

details of the re-analysis workflow, including ASV generation and phylogenetic inference, are provided in the Supporting Methods.

Formatted: Font: 10 pt

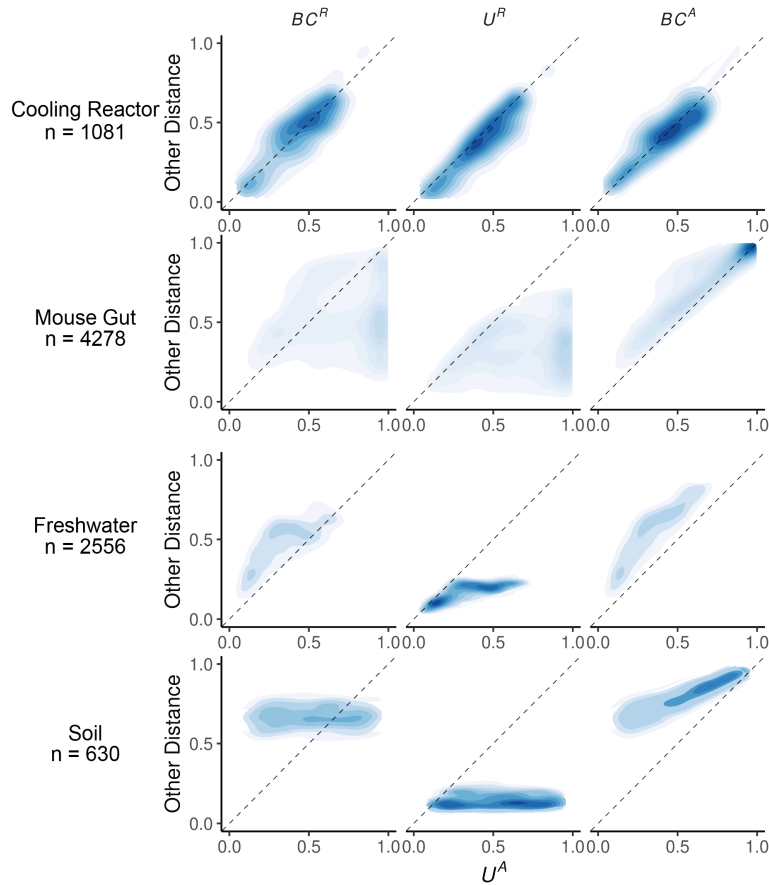
250
251
252
253
254
255
256

Figure 2. Absolute UniFrac (U^A) compared with other β -diversity metrics across four real microbial datasets. Each panel shows pairwise sample distances for U^A (x-axis) against another metric (y-axis): Bray-Curtis using relative abundance (BC^R , first column), weighted UniFrac using relative abundances (U^R , second column), and Bray-Curtis using absolute abundances (BC^A , third column). Contours indicate the relative density of pairwise comparisons (n shown for each dataset, left), with darker shading corresponding to more observations. The dashed line marks the 1:1 relationship. Points above the line indicate cases where U^A is smaller than the comparator metric, while points below the line indicate cases where U^A is larger.

Formatted: Indent: First line: 0", Line spacing: single

257
258
259
260

We first calculated four β -diversity metrics for all sample pairs in each dataset and compared them to U^A (Fig. 2). The degree of concordance between U^A and other metrics was highly context dependent. In the cooling water dataset, U^A closely tracked all three alternatives, whereas in the remaining systems it diverged substantially. U^A also spanned a similar or wider

Formatted: Font: 10 pt

Formatted: Line spacing: single

range of distances than the other metrics. For example, in the soil dataset BC^R and U^R occupied a narrow range relative to the broad separation observed under U^A .

U^A generally reported distances that were similar to or greater than U^R , consistent with the simulations shown in Fig. 1B. This reflects the ability of U^A to discern dissimilarity due to differences in microbial load, even when community composition is conserved. In contrast, U^A yielded distances that were similar to or lower than BC^A , again matching the simulated behavior in Fig 1B. In these cases, phylogenetic proximity between abundant, closely-related ASVs leads U^A to register greater similarity than BC^A .

Given these differences, we next quantified how well each metric discriminates among categorical sample groups. For each dataset, we ran PERMANOVAs to measure the proportion of variance (R^2) and statistical power (*pseudo-F*, *p-value*) attributable to group structure, using groupings that were determined to be significant in the original publications. To evaluate how strongly absolute abundance contributed to this discrimination, we also calculated GU^A across a range of α values. The resulting R^2 values are displayed in Fig. 3A, with the corresponding *pseudo-F* statistics and *p*-values provided in Fig. S2.

As in Fig. 2, the performance of each metric was strongly context dependent (Fig. 3A). In the mouse gut and freshwater datasets, absolute-abundance-aware metrics (BC^A and GU^A) explained the greatest proportion of variance (R^2), and R^2 generally increasing as α increased. In contrast, relative metrics captured more variation in the cooling water dataset (again at higher α), and all metrics explained comparably little variance in the soil dataset. Taken at face value, these trends might suggest that higher α values typically improve group differentiation.

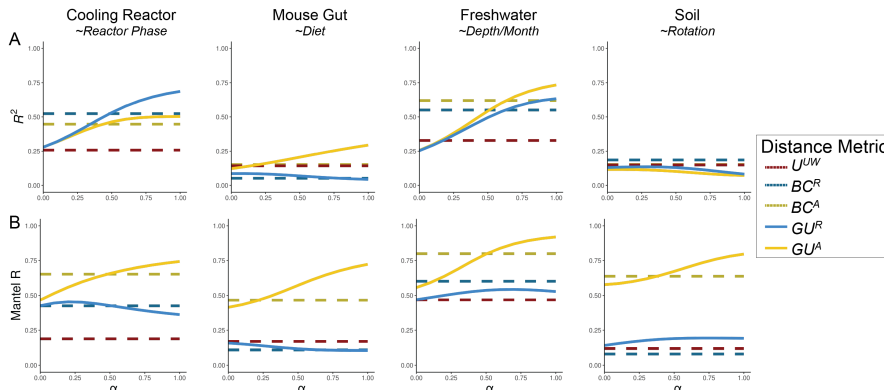
However, this comes with a major caveat: at high α values, GU^A becomes strongly correlated with total cell count alone (Fig. 3B). Mantel tests confirmed that absolute-abundance metrics are far more sensitive to differences in microbial load than their relative counterparts. This behavior is intuitive, and to some extent desirable, because these metrics are designed to detect changes in microbial load even when composition remains constant. Yet at $\alpha = 1$, U^A approaches a proxy for sample absolute abundance itself. In ordination space (Fig. S3), this can cause Axis 1 to correlate with absolute abundance and in some cases (freshwater and soil) produces strong horseshoe effects [15], potentially distorting ecological interpretation.

Deleted: integrates ecological realism by capturing differences in both lineage identity and total biomass.[¶]

Moved (insertion) [1]

Deleted: We next evaluated how U^A influences group separation in a real-world dataset. Using a previously published 16S rRNA gene dataset from Lake Ontario, we analyzed 66 samples and >7,000 ASVs. Samples clustered into three groups defined by depth and month, reflecting shifts in both taxonomic composition and microbial load (Fig. S2, [10]). Our goal was to determine whether weighting phylogenetic distances by absolute abundance enhances interpretability and statistical power to distinguish sample groups.[¶] with total cell count alone (Fig. 2D). Mantel tests showed that absolute distance metrics are much more sensitive to differences in cell counts than their relative counterparts. This is intuitive, and to a degree, intentional: these metrics aim to detect changes in biomass even when composition remains constant. Yet at $\alpha = 1$, U^A is nearly a proxy for sample biomass. In ordination space, this manifests as Axis 1 being almost perfectly correlated with absolute abundance (Spearman's $\rho = -1.0$), whereas at $\alpha = 0.0$, the correlation is moderate ($\rho = 0.58$). The structure observed in Fig. 2A at $\alpha = 1$ may largely reflect a horseshoe effect [14], where a strong gradient (here, cell counts) becomes curved in ordination space, potentially distorting ecological interpretation.[¶]

UniFrac (GU^A) across three levels of α : 0.0 (approximating unweighted UniFrac), 0.5, and 1.0 (equivalent to U^A). As α increased, PCoA ordinations revealed stronger similarity between Shallow May and Shallow September samples, reflecting their higher cell counts compared to the Deep samples (Fig. 2A). Notably, the proportion of variation explained by the first PCoA axis increased substantially with α , going from 18.3% at $\alpha = 0$ up to 76.7% $\alpha = 1$. This trend was also true for U^R across multiple α , but to a much weaker degree (Fig. S3).



327 **Figure 3. Discriminatory performance of U^A and related metrics across four microbial systems.** (A) PERMANOVAs
328 were used to quantify the percent variance (R^2) explained by predefined categorical groups (shown in italics beneath
329 each dataset name), with 1,000 permutations. PERMANOVA results were evaluated across five metrics and, where
330 applicable, across eleven α values (0-1 in 0.1 increments). For consistency with the original studies, only samples
331 from Reactor cycle 1 were used for the cooling-water dataset, only stool samples for the mouse gut dataset, and only
332 mature rhizosphere samples for the dataset. (B) Mantel correlation (R) between each distance metric and the
333 pairwise differences in absolute abundance (cell counts or 16S copy number), illustrating the degree to which each
334 metric is driven by biomass differences.

335 We recommend calibrating α based on research goals, modulating this effect by using
336 GU^A across a range of α rather than relying on U^A ($\alpha = 1$). Researchers should consider how
337 much emphasis they want their dissimilarity metric to place on microbial load (Box 1). When
338 biomass differences are central to the hypothesis being tested (for example, detecting
339 cyanobacterial blooms), high α are recommended. In contrast, if microbial load is irrelevant or
340 independent of the hypothesis in question, low α (or U^R) may be preferred; for example in the
341 soil dataset, fine-scale differences in composition may be obscured by random variation in
342 microbial load.

343 In many systems, microbial biomass is one piece of the story, likely correlated to other
344 variables being tested. If the importance of microbial load in the system is unknown, one
345 potential approach is to calculate correlations as demonstrated in Fig. 3B and select an α prior to
346 any ordinations or statistical testing. Again, correlation to cell count is valuable and is intrinsic to
347 absolute abundance-aware measures, especially when microbial load is relevant to the
348 hypotheses being tested. Correlations to cell count in BC^A , an accepted approach in the literature,
349 ranged from ~0.5 up to ~0.8. As a general recommendation from these analyses, we recommend
350 α values in an intermediate range from 0.1 up to 0.6, wherein GU^A has similar correlation to cell
351 count as BC^A .

352 Computational and Methodological Considerations

353 Applying GU^A in practice raises several considerations related to sequencing depth,
354 richness, and computational cost. Both Bray-Curtis and UniFrac can be sensitive to sequencing
355 depth because richness varies with read count [16–18]. Methods to address these concerns,
356 including rarefaction, remain debated and are challenging to benchmark rigorously [19]. We do
357 not evaluate the sensitivity of U^A or GU^A to different rarefaction strategies here, but we do

Formatted: Font: 10 pt

Formatted: Indent: First line: 0", Line spacing: single

Moved up [1]: at high α values, GU^A became strongly correlated with total cell count alone (Fig. 2D). Mantel tests showed that absolute distance metrics are much more sensitive to differences in cell counts than their relative counterparts. This is intuitive, and to a degree, intentional: these metrics aim to detect changes in biomass even when composition remains constant. Yet at $\alpha = 1$, U^A is nearly a proxy for sample biomass. In ordination space, this manifests as Axis 1 being almost perfectly correlated with absolute abundance (Spearman's $\rho = -1.0$), whereas at $\alpha = 0.0$, the correlation is moderate ($\rho = 0.58$). The structure observed in Fig. 2A at $\alpha = 1$ may largely reflect a horseshoe effect [12], where a strong gradient (here, cell counts) becomes curved in ordination space, potentially distorting ecological interpretation.

Deleted:

To quantify the impact on group differentiation, we performed PERMANOVA across depth-month groupings using GU^R , GU^A , BC^R , and BC^A at varying α (Fig. 2B–C). Across all metrics, incorporating absolute abundance increased both the proportion of explained variance (R^2) and the pseudo F -statistic. GU^A achieved a maximum R^2 of 75.8% and a pseudo F -statistic 1.56 times greater than GU^R , highlighting the ability of GU^A to detect group differences driven by microbial load.¹

However, a major caveat emerged:

Deleted:

Deleted: urge careful calibration of

Deleted: thereby mitigating

Formatted: Line spacing: single

Deleted:

Formatted: Indent: First line: 0.5", Line spacing: single

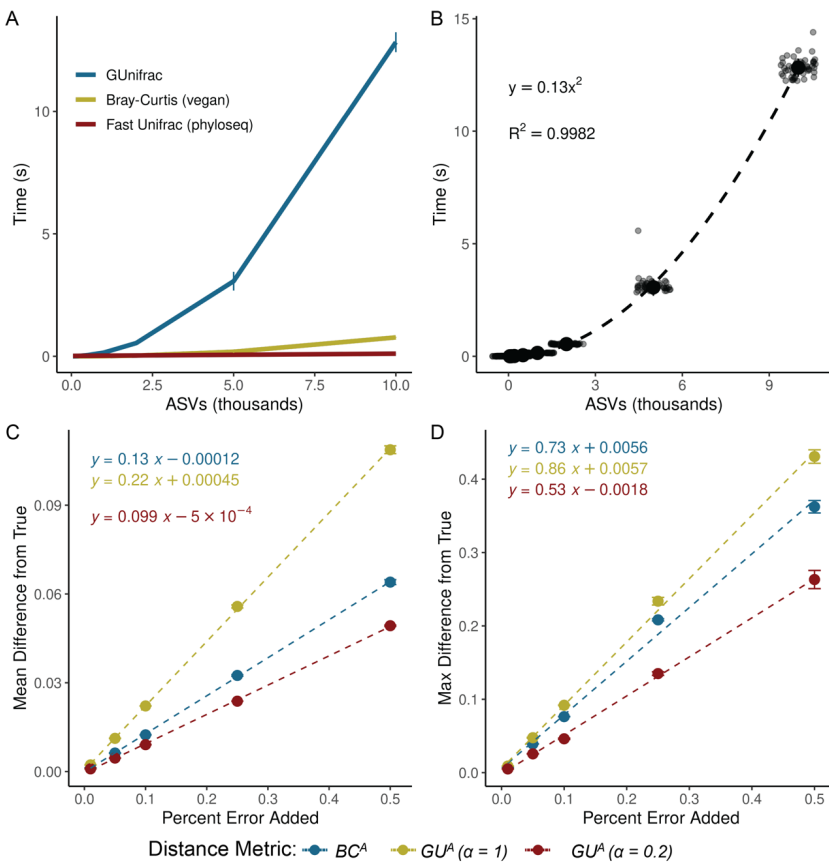
Deleted: In this dataset, we recommend an intermediate α of 0.5, consistent with prior guidance [9], but especially important when using absolute abundance data.

Deleted:

Formatted: Font: Bold

Formatted: Line spacing: single

431 provide a workflow and code for how we incorporated rarefaction into our own analyses (Box 2
 432 and available code). This approach minimizes sequencing-depth biases while preserving
 433 abundance scaling for downstream β -diversity analysis.



434

435 *Figure 4. GU^A requires more computational time but remains resilient to quantification error. (A) Runtime for GU^A*
 436 (*GUUnifrac package*), U^R (*FastUniFrac* in the *phyloseq* package) and BC^A (*vegan* package) was benchmarked across
 437 50 iterations on a sub-sampled soil dataset (mature samples only) [10], using increasing ASV richness (50, 100, 200,
 438 500, 1,000, 2,000, 5,000, 10,000), with 10 samples and one α value per run (unweighted UniFrac is also calculated
 439 by default). Error bars represent standard deviation. (B) Quadratic relationship between GU^A computation time and
 440 ASV richness. Large center point represents median across 50 iterations, error bars (standard deviation) are too
 441 small to be seen. (C-D) Sensitivity of GU^A ($\alpha = 1$ and 0.2) and BC^A to measurement error was evaluated by adding
 442 random variation ($\pm 1\%$ to $\pm 50\%$; Supporting Methods) to 16S copy number estimates in stool samples from the
 443 mouse gut dataset [3]. For each error level, 50 replicate matrices were generated and compared to the original
 444 values. Panels reflect the (C) mean difference and (D) max difference between the error-added metrics compared to
 445 the originals. Error bars represent the standard deviation of the average mean and max difference across 50
 446 iterations.

447 *GU^A* is slower to compute than both BC^A and U^R because it must traverse the phylogenetic
448 tree to calculate branch lengths for each iteration. Computational time of GU^A increases
449 quadratically with ASV number and is 10-20 times slower, though up to 50 times slower, than
450 BC^A (Fig. 4A-B). The number of samples or α values, however, have relatively little effect on
451 runtime (Fig. S4). For a dataset of 24,000 ASVs, computing on a single CPU is still reasonable
452 (1.4 minutes), but repeated rarefaction increases runtime substantially because branch lengths are
453 redundantly calculated with each iteration. Allowing branch-length objects to be cached or
454 incorporated directly into the GUnifrac workflow would considerably improve computational
455 efficiency.

456 We also evaluated the sensitivity of GU^A to measurement error in absolute abundance due to
457 uncertainty arising from the quantification of cell number of 16S copy number. To assess the
458 sensitivity of GU^A and BC^A to measurement error, we added random error to the 16S copy
459 number measurements from the mouse gut dataset, limiting our analyses to the stool samples
460 where copy numbers varied by an order of magnitude. Across 50 iterations, each copy number
461 could randomly vary by a given percentage of error in either direction. We re-calculated β -
462 diversity (BC^A and GU^A at $\alpha = 1$ and $\alpha = 0.2$) and compared these measurements to the original
463 dataset.

464 Introducing random variation into measured 16S copy number altered GU^A values only
465 modestly, and the effect was proportional to the magnitude of the added noise (Fig. 4C-D). At α
466 = 1, each 1% of quantification error introduced an average difference of 0.0022 in GU^A ; at $\alpha =$
467 0.2, GU^A was even less sensitive. Thus, moderate α values provide a balance between
468 interpretability and robustness to noise in absolute quantification. The max deviation from true
469 that added error could inflict on a given metric was also proportional (and always less) than the
470 magnitude of the error itself (Fig. 4D). A more rigorous approach to assessing error propagation
471 within these metrics, including mathematical proofs of the relationships estimated above, is
472 outside the scope of this paper but would be helpful.

473 Ecological Interpretation and conceptual significance

474 Absolute UniFrac reframes the interpretation of β -diversity by making biomass an explicit
475 ecological axis rather than an unmeasured or normalized-away quantity. Conventional UniFrac
476 captures composition and shared evolutionary history, but implicitly invites interpretation as if it
477 also encodes differences on microbial load. By incorporating absolute abundance directly,
478 Absolute UniFrac helps to resolve this mismatch and restores alignment between ecological
479 hypotheses and the quantities represented in the metric. In this view, β -diversity becomes a three-
480 axis ecological measure, incorporating composition, phylogeny and biomass, rather than a two-
481 axis approximation. That said, the additional dimension of microbial load also increases the
482 complexity of applying and interpreting this metric.

483 There are many cases where the incorporation of absolute abundance allows microbial
484 ecologists to assess more realistic, ecologically-relevant differences in microbial communities,
485 especially when microbial load is mechanistically central. Outside of the datasets re-analyzed
486 here [3, 5, 9, 10], the temporal development of the infant gut microbiome involves both a rise in
487 absolute abundance and compositional changes [6]; bacteriophage predation in wastewater
488 bioreactors can be understood only when microbial load is considered [20]; and antibiotic-driven
489 declines in specific swine gut taxa were missed using relative abundance approaches [21]. As β -

Formatted: Indent: First line: 0.5", Space After: 8 pt,
Adjust space between Latin and Asian text, Adjust space
between Asian text and numbers, Tab stops: Not at 0.39" +
0.78" + 1.17" + 1.56" + 1.94" + 2.33" + 2.72" + 3.11" +
3.5" + 3.89" + 4.28" + 4.67"

Formatted: Font: Not Italic

Formatted: Font: Not Italic

Formatted: Font: (Default) Times New Roman

Formatted: Font: (Default) Times New Roman

Formatted: Font: (Default) Times New Roman

Formatted: Line spacing: single

Formatted: Font: (Default) Times New Roman

Formatted: Font: (Default) Times New Roman

Formatted: No underline

Formatted: Indent: First line: 0.35", Line spacing: single

Formatted: Font: 10 pt

Deleted: [11][3]

491 diversity metrics (and UniFrac specifically) remain central to microbial ecology, these findings
492 highlight how interpretation changes once biomass is incorporated. Broader adoption of absolute
493 abundance profiling will also depend on data availability. Few studies currently make absolute
494 quantification data publicly accessible, underscoring the need to deposit absolute measurements
495 alongside sequencing reads for reproducibility, ideally as metadata within SRA submissions.

496 While demonstrated here with 16S rRNA data, the approach should extend to other marker
497 genes or (meta)genomic features, provided absolute abundance estimates are available. In this
498 sense, GU^A offers a more ecologically grounded view of lineage turnover by jointly reflecting
499 variation in biomass and phylogenetic structure.

500 No single metric (or α in GU^A), however, is universally “best”. Each β -diversity metric
501 emphasizes a different dimension of community change. Researchers should therefore select
502 metrics based on the ecological quantity that is hypothesized to matter most (Box 1). Here, we
503 demonstrate not that GU^A outperforms other measures, but that it faithfully incorporates the three
504 axes of variation it was designed to incorporate: composition, phylogenetic similarity, and
505 absolute abundance (Fig. 1 and Fig. 2). As with any β -diversity analysis, interpretation requires
506 matching the metric to the ecological question at hand, and exploring sensitivity across different
507 metrics where appropriate [22]. By providing demonstrations and code for the application and
508 interpretation of U^A/GU^A , we hope to encourage the use of these metrics as a tool of microbial
509 ecology.

510 Conclusion

511 By explicitly incorporating absolute abundance, Absolute UniFrac shifts phylogenetic β -
512 diversity from a two-axis approximation to a three-axis ecological measure. This reframing
513 connects the metric to the underlying biological questions that motivate many microbiome
514 studies. As methods for quantifying microbial load continue to expand, the ability to interpret β -
515 diversity in a biomass-aware framework will become increasingly important for distinguishing
516 true ecological turnover from proportional change alone. In this way, Absolute UniFrac is not
517 simply an alternative distance metric but a tool for aligning statistical representation with
518 ecological mechanism.

519

Formatted: Indent: First line: 0.35", Line spacing: single

Deleted:

Formatted: Line spacing: single

Formatted: Font: Not Italic

522 **Box 1: β -diversity metrics should reflect the hypothesis being tested**

Formatted: Font: Bold

523 Absolute UniFrac is most informative when variation in microbial load is expected to carry
 524 ecological meaning rather than being a nuisance variable. The choice of α determines how
 525 strongly abundance differences influence the metric, and should therefore be selected based on
 526 the hypothesis, not by convention. In settings where biomass is central to the mechanism under
 527 study, higher α values appropriately foreground that signal, whereas in cases where load
 528 variation is incidental or confounding, lower α values maintain interpretability. Framing α as a
 529 hypothesis-driven choice repositions β -diversity from a default normalization step to an explicit
 530 ecological decision.

			Metric to Use			Hypothetical Example
Treat closely related lineages as similar?	Yes	How relevant is microbial load?	Central to hypothesis			<i>GU^A, $\alpha > 0.5$</i>
			Relevant, but associated with other variables of interest			<i>GU^A, $0.1 < \alpha < 0.5$</i>
			Irrelevant	Emphasize rare or dominant taxa?	Dominant	<i>GU^R, $\alpha > 0.5$</i>
					Rare	<i>GU^R, $\alpha < 0.5$</i>
			Unknown			<i>GU^A at multiple α</i>
	No	Microbial load relevant?	Yes		<i>BC^A</i>	Random variation in microbial load obscured compositional shifts in soil communities
	No		<i>BC^R</i>	Strain turnover and proliferation in the infant gut		
				Temporal succession in chemostat		

Formatted: Font: 10 pt

Formatted: Font: 10 pt

Formatted: Centered

Formatted: Font: 10 pt

Formatted: Font: 10 pt

Formatted: Centered

Formatted: Font: 10 pt, Not Italic

Formatted: Font: 10 pt

Formatted: Centered

533

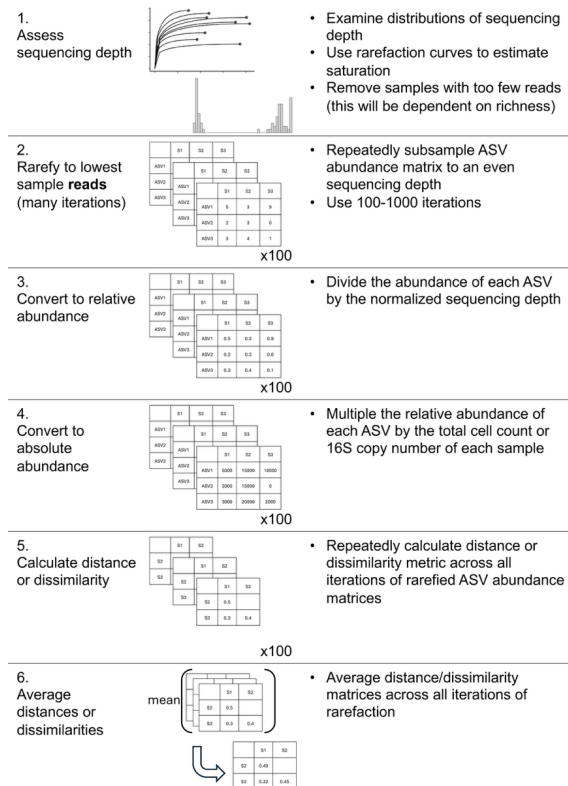
534 **Box 2: Rarefaction workflow for incorporating absolute abundance**

Formatted: Font: Bold

535 While we refrain from an in-depth
 536 analysis of rarefaction approaches,
 537 here we present our workflow for
 538 incorporating rarefaction alongside
 539 absolute abundance. First, samples
 540 were assessed for anomalously low
 541 read counts and discarded
 542 (sequencing blanks and controls
 543 were also removed). For rarefaction,
 544 each sample in the ASV table was
 545 subsampled to equal sequencing
 546 depth (# of reads) across 100
 547 iterations, creating 100 rarefied ASV
 548 tables. These tables were then
 549 converted to relative abundance by
 550 dividing each ASV's count by the
 551 equal sequencing depth (rounding
 552 was not performed). Then, each
 553 ASV's absolute abundance within a
 554 given sample was calculated by
 555 multiplying its relative abundance
 556 by that sample's total cell count or
 557 16S copy number. Methods to
 558 predict genomic 16S copy number
 559 for a given ASV were not used [23].

560 Each distance/dissimilarity metric was then calculated across all 100 absolute-normalized ASV
 561 tables. The final distance/dissimilarity matrix was calculated by averaging all 100 iterations of
 562 each distance/dissimilarity calculation. Of note for future users: pruning the phylogenetic tree
 563 after rarefaction for each iteration is not necessary – ASVs removed from the dataset do not
 564 contribute nor change the calculated UniFrac distances.

565



566

567

568 **References**

- 569 1. Gloor GB et al. Microbiome Datasets Are Compositional: And This Is Not Optional. *Front
570 Microbiol* 2017;8:2224. <https://doi.org/10.3389/fmicb.2017.02224>
- 571 2. Vandepitte D et al. Stool consistency is strongly associated with gut microbiota richness
572 and composition, enterotypes and bacterial growth rates. *Gut* 2016;65:57–62.
573 <https://doi.org/10.1136/gutjnl-2015-309618>
- 574 3. Barlow JT, Bogatyrev SR, Ismagilov RF. A quantitative sequencing framework for absolute
575 abundance measurements of mucosal and luminal microbial communities. *Nat Commun*
576 2020;11:2590. <https://doi.org/10.1038/s41467-020-16224-6>
- 577 4. Wang X et al. Current Applications of Absolute Bacterial Quantification in Microbiome
578 Studies and Decision-Making Regarding Different Biological Questions. *Microorganisms*
579 2021;9:1797. <https://doi.org/10.3390/microorganisms9091797>
- 580 5. Props R et al. Absolute quantification of microbial taxon abundances. *ISME J* 2017;11:584–
581 587. <https://doi.org/10.1038/ismej.2016.117>
- 582 6. Rao C et al. Multi-kingdom ecological drivers of microbiota assembly in preterm infants.
583 *Nature* 2021;591:633–638. <https://doi.org/10.1038/s41586-021-03241-8>
- 584 7. Bray JR, Curtis JT. An Ordination of the Upland Forest Communities of Southern
585 Wisconsin. *Ecological Monographs* 1957;27:326–349. <https://doi.org/10.2307/1942268>
- 586 8. Lozupone CA et al. Quantitative and Qualitative β Diversity Measures Lead to Different
587 Insights into Factors That Structure Microbial Communities. *Applied and Environmental
588 Microbiology* 2007;73:1576–1585. <https://doi.org/10.1128/AEM.01996-06>

Formatted: Line spacing: single

Deleted: That said, interpretation of GU^A requires care. When biomass differences dominate, ordinations may largely reflect microbial load rather than lineage turnover, particularly at $\alpha = 1$ and with long phylogenetic branches. In such cases, higher statistical power may come at the cost of biological nuance. We also do not address related concerns, such as how sequencing depth influences richness estimates or whether rarefaction should be applied before calculating GU^A [15]. As with any β -diversity study, researchers should interpret results critically, explore sensitivity across metrics, and justify their choice of α [16]. Our results suggest that an intermediate α value offers a practical compromise that balances sensitivity to biomass with robustness to overdominance by total load, especially when lineage turnover is also of interest. We anticipate that GU^A will become an essential tool for microbiome researchers seeking to incorporate absolute abundance into ecologically grounded β -diversity comparisons.¶

- 607 9. Pendleton A, Wells M, Schmidt ML. Upwelling periodically disturbs the ecological
608 assembly of microbial communities in the Laurentian Great Lakes. 2025. bioRxiv, 2025. ,
609 2025.01.17.633667
- 610 10. Zhang K et al. Absolute microbiome profiling highlights the links among microbial
611 stability, soil health, and crop productivity under long-term sod-based rotation. *Biol Fertil
612 Soils* 2022;58:883–901. <https://doi.org/10.1007/s00374-022-01675-4>
- 613 11. Chen J et al. Associating microbiome composition with environmental covariates using
614 generalized UniFrac distances. *Bioinformatics* 2012;28:2106–2113.
615 <https://doi.org/10.1093/bioinformatics/bts342>
- 616 12. Lozupone C, Knight R. UniFrac: a New Phylogenetic Method for Comparing Microbial
617 Communities. *Applied and Environmental Microbiology* 2005;71:8228–8235.
618 <https://doi.org/10.1128/AEM.71.12.8228-8235.2005>
- 619 13. McMurdie PJ, Holmes S. phyloseq: An R package for reproducible interactive analysis and
620 graphics of microbiome census data. *PLoS ONE* 2013;8:e61217.
- 621 14. Bolyen E et al. Reproducible, interactive, scalable and extensible microbiome data science
622 using QIIME 2. *Nat Biotechnol* 2019;37:852–857. [https://doi.org/10.1038/s41587-019-0209-9](https://doi.org/10.1038/s41587-019-
623 0209-9)
- 624 15. Morton JT et al. Uncovering the Horseshoe Effect in Microbial Analyses. *mSystems*
625 2017;2:10.1128/msystems.00166-16. <https://doi.org/10.1128/msystems.00166-16>
- 626 16. Schloss PD. Evaluating different approaches that test whether microbial communities have
627 the same structure. *The ISME Journal* 2008;2:265–275.
628 <https://doi.org/10.1038/ismej.2008.5>

- 629 17. Fukuyama J et al. Comparisons of distance methods for combining covariates and
630 abundances in microbiome studies. *Biocomputing* 2012. WORLD SCIENTIFIC, 2011,
631 213–224.
- 632 18. McMurdie PJ, Holmes S. Waste Not, Want Not: Why Rarefying Microbiome Data Is
633 Inadmissible. *PLOS Computational Biology* 2014;10:e1003531.
634 <https://doi.org/10.1371/journal.pcbi.1003531>
- 635 19. Schloss PD. Waste not, want not: revisiting the analysis that called into question the
636 practice of rarefaction. *mSphere* 2023;9:e00355-23. <https://doi.org/10.1128/mSphere.00355-23>
- 637 20. Shapiro OH, Kushmaro A, Brenner A. Bacteriophage predation regulates microbial
638 abundance and diversity in a full-scale bioreactor treating industrial wastewater. *The ISME
639 Journal* 2010;4:327–336. <https://doi.org/10.1038/ismej.2009.118>
- 640 21. Wagner S et al. Absolute abundance calculation enhances the significance of microbiome
641 data in antibiotic treatment studies. *Front Microbiol* 2025;16.
642 <https://doi.org/10.3389/fmicb.2025.1481197>
- 643 22. Kers JG, Saccenti E. The Power of Microbiome Studies: Some Considerations on Which
644 Alpha and Beta Metrics to Use and How to Report Results. *Front Microbiol* 2022;12.
645 <https://doi.org/10.3389/fmicb.2021.796025>
- 646 23. Douglas GM et al. PICRUSt2 for prediction of metagenome functions. *Nat Biotechnol*
647 2020;38:685–688. <https://doi.org/10.1038/s41587-020-0548-6>
- 648
- 649

Page 9: [1] Deleted

Augustus Raymond Pendleton

9/28/25 9:44:00 PM